NON-EQUILIBRIUM H₂ FORMATION IN THE EARLY UNIVERSE: ENERGY EXCHANGES, RATE COEFFICIENTS AND SPECTRAL DISTORTIONS

C. M. Coppola[1,2], R. D'Introno[3], D. Galli[4], J. Tennyson[2], S. Longo[1,5]

Draft version November 24, 2013

ABSTRACT

Energy exchange processes play a crucial role in the early Universe, affecting the thermal balance and the dynamical evolution of the primordial gas. In the present work we focus on the consequences of a non-thermal distribution of the level populations of H₂: first, we determine the excitation temperatures of vibrational transitions and the non-equilibrium heat transfer; second, we compare the modifications to chemical reaction rate coefficients with respect to the values obtained assuming local thermodynamic equilibrium; third, we compute the spectral distortions to the cosmic background radiation generated by the formation of H₂ in vibrationally excited levels. We conclude that non-equilibrium processes cannot be ignored in cosmological simulations of the evolution of baryons, although their observational signatures remain below current limits of detection. New fits to the equilibrium and non-equilibrium heat transfer functions are provided.

Subject headings: molecular processes; cosmology: early Universe, cosmic microwave background

1. INTRODUCTION

Understanding the thermal evolution of the Universe in the epoch in which atoms and molecules formed is a crucial step to properly model the birth of the first bound structures (e.g., Flower & Pineau des Forêts 2001). In particular, the balance between cooling and heating processes has to be taken into account and modeled according to the chemical and physical processes occuring in the primordial plasma. It is well established that Lyman-α cooling is effective at gas temperature higher than ∼ 8000 K, corresponding to redshifts $z \gtrsim 2700$, while primordial molecules, in particular H₂ and HD formed at $z \lesssim 1000$, are the most efficient cooling agents of the pristine plasma at lower temperatures.

Several authors have calculated the heating and cooling functions of the primordial molecular species: Palla et al. (1983), Lepp & Shull (1984), Puy et al. (1993), Le Bourlot et al. (1999), Puy & Signore (1996), Galli & Palla 1998 (hereafter GP98), Coppola et al. (2011b). One of the standard assumptions in these calculations is that the population of internal states can be described by a Boltzmann distribution. This hypothesis is valid in many astrophysical environments where the density is sufficiently high to bring the internal degrees of freedom to a condition of local thermodynamic equilibrium (LTE). For a given species, e.g. H₂, this condition is quantified in terms of a critical density $n_{cr}(H)$ defined as the ratio between radiative and collisional de-excitation coefficients of H₂. It is easy to check that even at highest redshifts ($z \approx 1000$), the ambient baryon density n_b is ∼ 2 orders of magnitude below the critical density $n_{cr}(H)$

Electronic address: carla.coppola@chimica.uniba.it

[1] Università degli Studi di Bari, Dipartimento di Chimica, Via Orabona 4, I-70126 Bari, Italy
[2] Department of Physics and Astronomy, University College London, Gower Street, London WC1E 6BT
[3] Università degli Studi di Bari, Dipartimento di Fisica, Via Amendola 173, I-70126 Bari, Italy
[4] INAF-Osservatorio Astrofisico di Arcetri, Largo E. Fermi 5, I-50125 Firenze, Italy
[5] IMIP-CNR, Section of Bari, via Amendola 122/D, I-70126 Bari, Italy

(although considering specific rotational transitions the critical density is below the baryon one up to lower redshift $z \approx 500$). In addition, several physical phenomena (e.g. shocks) and chemical processes can produce deviations from LTE. In particular, most of the gas-phase molecular formation processes selectively produce species in states that deviate significantly from LTE.

In the case of the early Universe, Coppola et al. (2011a) (hereafter C11) computed the vibrational distribution of H₂ and H₂⁺ formed at redshifts $10 < z < 1000$ and found that high sovrathermal tails are present especially at low z. The existence of non-equilibrium features in the level populations of H₂ is important, because of the role of this species as a coolant of primordial gas. In the present work, we extend the work of C11 to study the following physical quantities relevant to the non-equilibrium energy exchange in the primordial Universe: excitation temperatures, heat transfer functions, reaction rates and spectral distortions of cosmic background radiation (CBR).

2. REDUCED MODEL: ORTHO- AND PARA- STATES

Because the number of roto-vibrational levels involved in the kinetics of H₂ is too high (≈ 300) for a direct extension of the approach used by C11, in the present work we implement a reduced model in order to provide a simpler starting point for more extended calculations. This model is based on the assumptions that: (1) the most important channels determining the population of vibrational states are the associative detachment reaction

$$H^- + H \rightarrow H_2 + e,$$
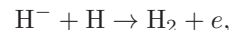
and the spontaneous and stimulated radiative transitions between roto-vibrational levels; and (2) a steady-state approximation can be applied to the kinetics of vibrational levels. Under these hypotheses, two steady-state Master Equations (for ortho- and para- states, respectively) can be written for the 15 vibrational levels ($i = 0, 14$) of H₂:

$$f_i \sum_{j, i \neq j} R_{ij} - \sum_{j, i \neq j} R_{ji} f_j = k_i f_{H^-} f_H n_b, \quad (1)$$

where f_i is the fractional abundance of H_2 in the ith level, f_{H^-} and f_H those of H^- and H respectively, R_{ij} is the matrix of radiative coefficients including absorption processes, calculated as in C11 averaging over the initial rotational levels and summing over the final ones the Einstein coefficients computed by Wolniewicz et al. (1998). The values of f_{H^-} and f_H are taken from the complete kinetic model by C11. The rate coefficients k_i for the associative detachment reaction for the ith vibrational level formation have been evaluated using the cross-sections σ_{ij} calculated by Čížek et al. (1998) summing over all final rotational states:

$$k_i(T_{\text{m}}) = \sum_{j=0}^{j_{\text{max}}(i)} \tilde{k}_{ij}(T_{\text{m}}), \qquad (2)$$

where

$$\tilde{k}_{ij}(T_{\text{m}}) = \sqrt{\frac{8}{\pi\mu(k_{\text{B}}T_{\text{m}})^3}} \int_0^\infty E\,\sigma_{ij}(E)e^{-E/(k_{\text{B}}T_{\text{m}})}\,dE, \qquad (3)$$

with μ reduced mass of the system and T_{m} matter temperature. It should be noted that experimental results by Kreckel et al. (2010) recently showed very good agreement with these quantum calculations.

The equation for the vibrational ground state f_0 in Eq. 1 is replaced by the normalization condition

$$\sum_i f_i = f_{H_2}, \qquad (4)$$

where $f_{H_2}(z)$ is the fraction of H_2 which is also taken from the complete model. Figure 1 shows the fractional abundance of vibrational levels obtained using the reduced model described in the present section. The results for all f_i are satisfactory close to those obtained with the fully kinetic model shown in Figure 10 of C11, at least for not too high values of z. These results show that the hypothesis of steady-state can be applied to the present problem with enough confidence to proceed to the study of the ortho- and para- states. For this we calculate two sets of rate coefficients $k_{i,\text{ortho}}(T_{\text{m}})$ and $k_{i,\text{para}}(T_{\text{m}})$ for each vibrational level i,

$$k_{i,\text{ortho}}(T_{\text{m}}) = \sum_{j\text{ odd}} \tilde{k}_{ij}(T_{\text{m}}),$$
$$k_{i,\text{para}}(T_{\text{m}}) = \sum_{j\text{ even}} \tilde{k}_{ij}(T_{\text{m}}). \qquad (5)$$

The R_{ij} coefficients are also thermally averaged over a partial distribution. The first equation of each system is replaced by the normalization condition

$$\sum_i f_{i,\text{ortho/para}} = 1, \qquad (6)$$

which means that we are calculating the vibrational distribution of each of the two species but not the total fraction of ortho- and para- hydrogen, which cannot be calculated by a steady-state approach.

3. EXCITATION TEMPERATURES

For each transition 0–v, the excitation temperature is defined as

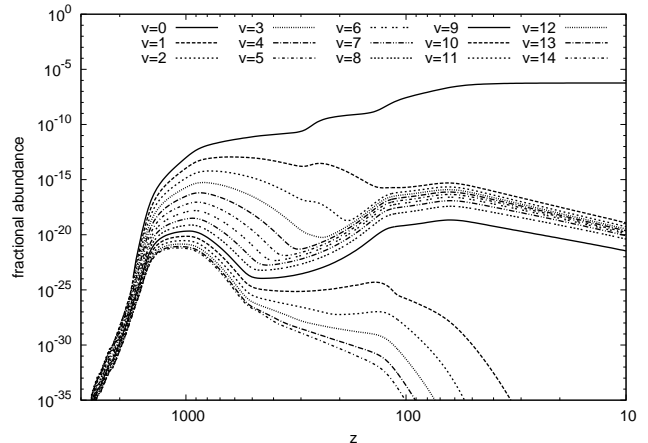$$T_{0-v} = \frac{E_v - E_0}{k_{\text{B}}\ln(n_0/n_v)}, \qquad (7)$$

Fig. 1.— Fractional abundances of the vibrational levels of H_2 according to the reduced steady-state model described in the text.

where E_v and n_v represent the energy and fractional abundance of the vth vibrational level, respectively, and k_{B} is the Boltzmann constant.

In Figure 2, the excitation temperature of the transitions $0 - v$ is compared to the temperatures of matter and radiation as a function of z. For better clarity, a few curves have been repeated in the two panels. The figure shows that vibration decouples from the translational motion, and this happens at higher z than the decoupling of radiation and matter; for the most excited levels this corresponds to an epoch where the conditions are near equilibrium. Later, after the decoupling of matter and radiation, T_{0-1} is slightly larger than the radiation temperature T_{r}; the excitation temperatures T_{0-v} for higher v are progressively higher. This result can be explained by considering the reaction network: the vibrational levels are formed by associative reactions that preferentially populate highly excited levels, while the vibrational manifold as a whole is coupled to the CBR (which provides a heat sink) much better than to the matter; this latter coupling occurs via the relatively ineffective H_2/H VT processes. Therefore, all levels pairs are expected to be warmer than the radiation field, but the lowest pairs are closer to equilibrium with the radiation because the chemical heating is lower.

The separation of T_{0-1} and T_{r} occurs at $z \approx 100$, which brings this phenomenon not far from potential indirect observation (e.g. effects on reaction rates of processes and consequent different fractional abundances of chemical species at lower z). Another relevant feature of our calculation is that T_{0-1} is stable at about 200 K at the age of formation of the first structures. Since the $1 \rightarrow 0$ transition is an important heat radiator, our results indicate that T_{0-1} is a more appropriate initial condition for the vibrational temperature of H_2 in hydrodynamic collapse models than T_{r}, which is considerably lower. In Table 1 the values for z_{dec} (redshift at which excitation temperature decouples from radiation temperature) and $z_{\text{freeze-out}}$ (redshift at which the freeze-out temperature is reached) are reported for each T_{0-i}; the former are evaluated considering a relative deviation from T_{r} larger than 1%, while the latter are calculated searching for relative deviation of T_{0-i} at each z from the value at $z = 10$ smaller than 10^{-3}.
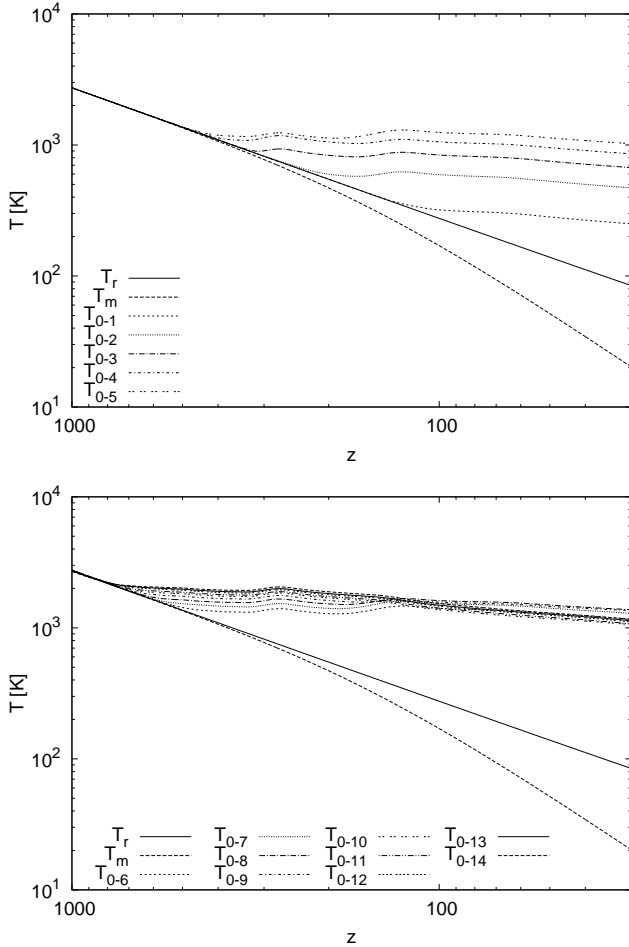
Figure 3 shows the values of the relative difference be-

Fig. 2.— H₂ excitation temperatures T_{0-v}, compared to the temperature of the radiation (*solid curve*) and matter (*dashed curve*). *Top panel*: $v = 1$ to $v = 5$; *bottom panel*: $v = 6$ to $v = 14$.

Fig. 3.— Ratio of excitation temperatures for ortho- and para-states given as $(T_{0-i,\mathrm{ortho}} - T_{0-i,\mathrm{para}})/T_{0-i,\mathrm{ortho}}$. *Top panel*: $v = 1$ to $v = 8$; *bottom panel*: $v = 9$ to $v = 14$.

TABLE 1
DECOUPLING REDSHIFT OF EXCITATION TEMPERATURES

Excitation temperature (K)	z_{dec}	$z_{\mathrm{freeze-out}}$
T_{0-14}	697	382
T_{0-13}	689	379
T_{0-12}	676	377
T_{0-11}	647	379
T_{0-10}	627	382
T_{0-9}	593	537
T_{0-8}	551	524
T_{0-7}	511	389
T_{0-6}	457	389
T_{0-5}	391	377
T_{0-4}	363	346
T_{0-3}	300	313
T_{0-2}	198	174
T_{0-1}	108	84

tween the vibrational excitation temperatures of ortho- and para- states. As can be seen, significant deviations between vibrational temperature of states with different rotational symmetry can be detected at low z and high i. These differences suggest that the issue of rotational non-equilibrium could be important and deserves to be
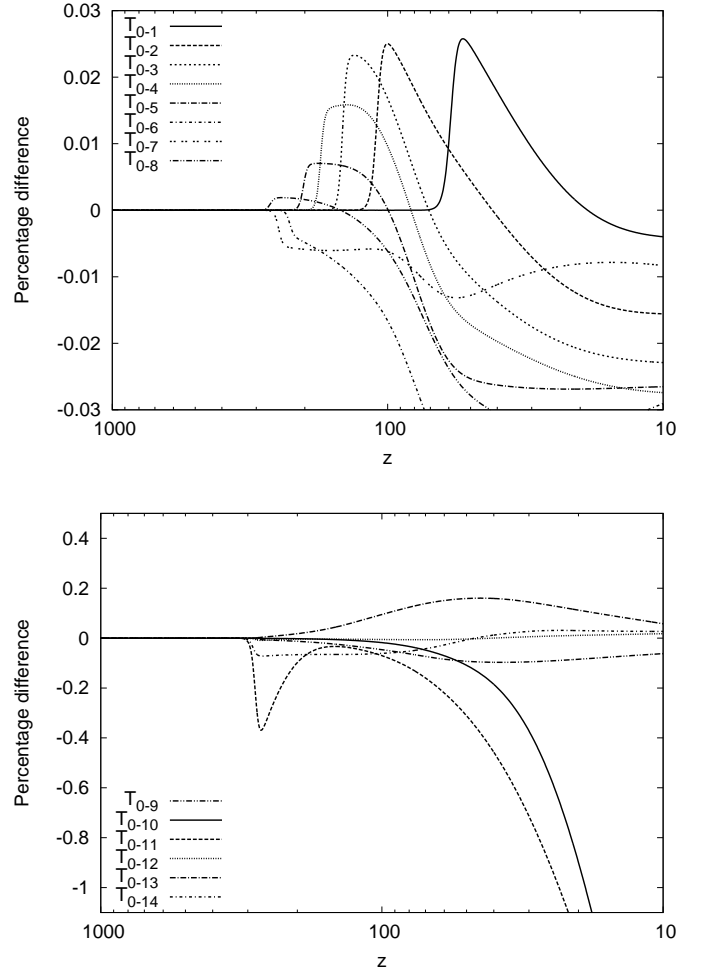
addressed accurately in future studies, i.e. by solving the Master Equation for a full rotovibrational manifold.

4. HEAT TRANSFER FUNCTION

In this paper we discuss the role of chemical energy from exothermic reaction, which is ultimately dissipated either into radiation or into the thermal energy of H atoms. This energy flow is described by heating and cooling functions, usually indicated with the symbols Γ and Λ, respectively. We consider the net molecular heat transfer, defined as the sum of all radiative excitations of H₂ followed by collisional de-excitations with H atoms and all collisional excitations followed by radiative decay:

$$\Phi(T_{\mathrm{m}}, T_{\mathrm{r}}) = (\Gamma - \Lambda)_{\mathrm{H_2}} = \frac{1}{n(\mathrm{H_2})} \times$$
$$\sum_{(v',j')<(v,j)} (n_{(v',j')}(T_{\mathrm{r}}) \cdot k_{(v',j')\to(v,j)}(T_{\mathrm{m}}) \qquad (8)$$
$$- n_{(v,j)}(T_{\mathrm{r}}) \cdot k_{(v,j)\to(v',j')}(T_{\mathrm{m}})(E_{v,j} - E_{v',j'}),$$

where T_{m} and T_{r} are the temperatures of matter and radiation, $k_{(v',j')\to(v,j)}$ is the VT (vibrational-translational) rate coefficient for H+H₂$(v',j') \to$ H+H₂(v,j), and $n_{(v,j)}$ describes the distribution of ro-

tovibrational levels,

$$n_{(v,j)}(T_{\mathrm{r}}) = \frac{g_j n_v (2j+1) \exp\left(-\frac{E_{v,j}-E_{v,0}}{k_{\mathrm{B}}T_{\mathrm{r}}}\right)}{Z_v(T_{\mathrm{r}})}, \quad (9)$$

with g_j equal to 1/4 and 3/4 for the para- and ortho-states, respectively, and $Z_v(T_{\mathrm{r}})$ rotational partition function for the vth level. It can be seen from Eqs. (8)-(9) that the rotational energy is distributed according to the Boltzmann law with temperature T_{r} while VT co-efficients depend on the matter temperature T_{m}. Thus, the heat transfer function depends on two temperatures, as a consequence of the different couplings of the internal degrees of freedom of molecules with the radiation and the matter: a faster coupling occuring between radiation and rotation, a slower coupling between translation and vibration.

We explore both equilibrium and non-equilibrium cases, corresponding to different values of n_v; in the former case the vibrational levels are distributed following the Boltzmann population equation, whereas in the latter we adopt the level populations resulting from the kinetic model of C11. VT rate coefficients have been taken from Esposito et al. (1999, 2001). These coefficients are given as functions of the initial and final rotovibrational quantum numbers and of temperature allowing the inclusion of the full sets of collisional transitions in our calculation. The equilibrium one-temperature heat transfer using the same rate coefficients has been compared with the analytical expression for the cooling function given by GP98. In GP98, the gas was not embedded in any radiation field; consequently, only collisional de-excitations were considered.

As it can be seen from Figure 4, the non-equilibrium heat transfer function decreases more rapidly than the equilibrium one at lower temperature, because of the increased efficiency in the energy exchange due to the long sovrathermal tails in the vibrational distribution. In the two temperatures calculation, the deviation is amplified as a consequence of the strong decoupling in the energy exchange among degrees of freedom and of the different trend of the gas and radiation temperatures. The first effect, which is due to the deviation of the vibrational population from the equilibrium distribution (essentially those of the lowest levels) is seen at $z \approx 1000$, and amounts to a factor of ~ 2. The effect of the separation of T_{m} and T_{r} occurs at low z where these two temperatures are considerably different. Consequently, in the computation of the heat transfer function at least two temperatures must be used: one is the temperature of the level population and the other is the translational temperature. This difference is evident in Eq. (8).

All heat transfer functions available in the literature are calculated assuming a single temperature, usually set equal to T_{r}. Such usage cannot capture the second non-equilibrium effect described above, since $k(T_{\mathrm{m}}, T_{\mathrm{r}})$ is implicitly set equal to $k(T_{\mathrm{r}})$. A better solution is to use in the context of early Universe models heat transfer functions calculated including non-equilibrium effects although fitted later as a function of a single temperature. Fits for the non-equilibrium case using the present two-temperatures model and the equilibrium case using the newest available data by Esposito et al. (1999, 2001) are
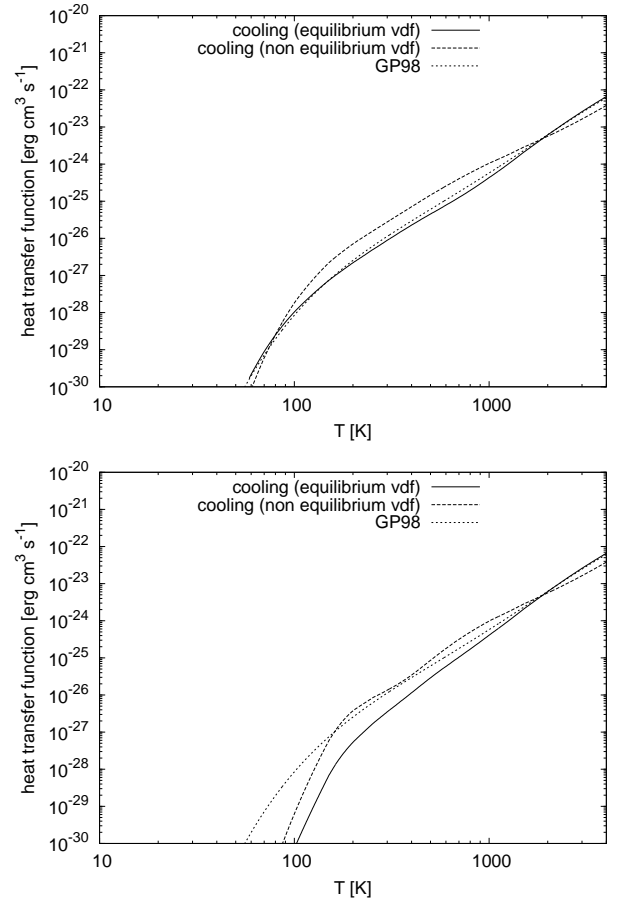

FIG. 4.— Heat transfer function $(\Gamma - \Lambda)_{\mathrm{H}_2}$ as a function of the radiation temperature T_{r}. *Dotted line*: GP98 fit for the cooling function; *solid line*: LTE calculation with present VT coefficients; *dashed line*: non-equilibrium vibrational distribution contribution. Calculation are reported both in the one-temperature case (*top panel*) and the two-temperatures one (*bottom panel*).

TABLE 2
H_2 HEAT TRANSFER FUNCTION

	Fitting coefficients
equilibrium	$a_0 = -145.05$
	$a_1 = 136.085$
	$a_2 = -58.6885$
	$a_3 = 11.2688$
	$a_4 = -0.786142$
non-equilibrium	$a_0 = -393.441$
	$a_1 = 588.474$
	$a_2 = -380.78$
	$a_3 = 123.858$
	$a_4 = -20.1349$
	$a_5 = 1.30753$

obtained in the form:

$$\log_{10} \Phi = \sum_{n=0}^{N} a_n (\log_{10} T_{\mathrm{r}})^n. \quad (10)$$

The coefficients a_n are listed in Table 2. For the non-equilibrium case, the validity of the fit is up to $T \approx 100$ K (additional data are available upon request).
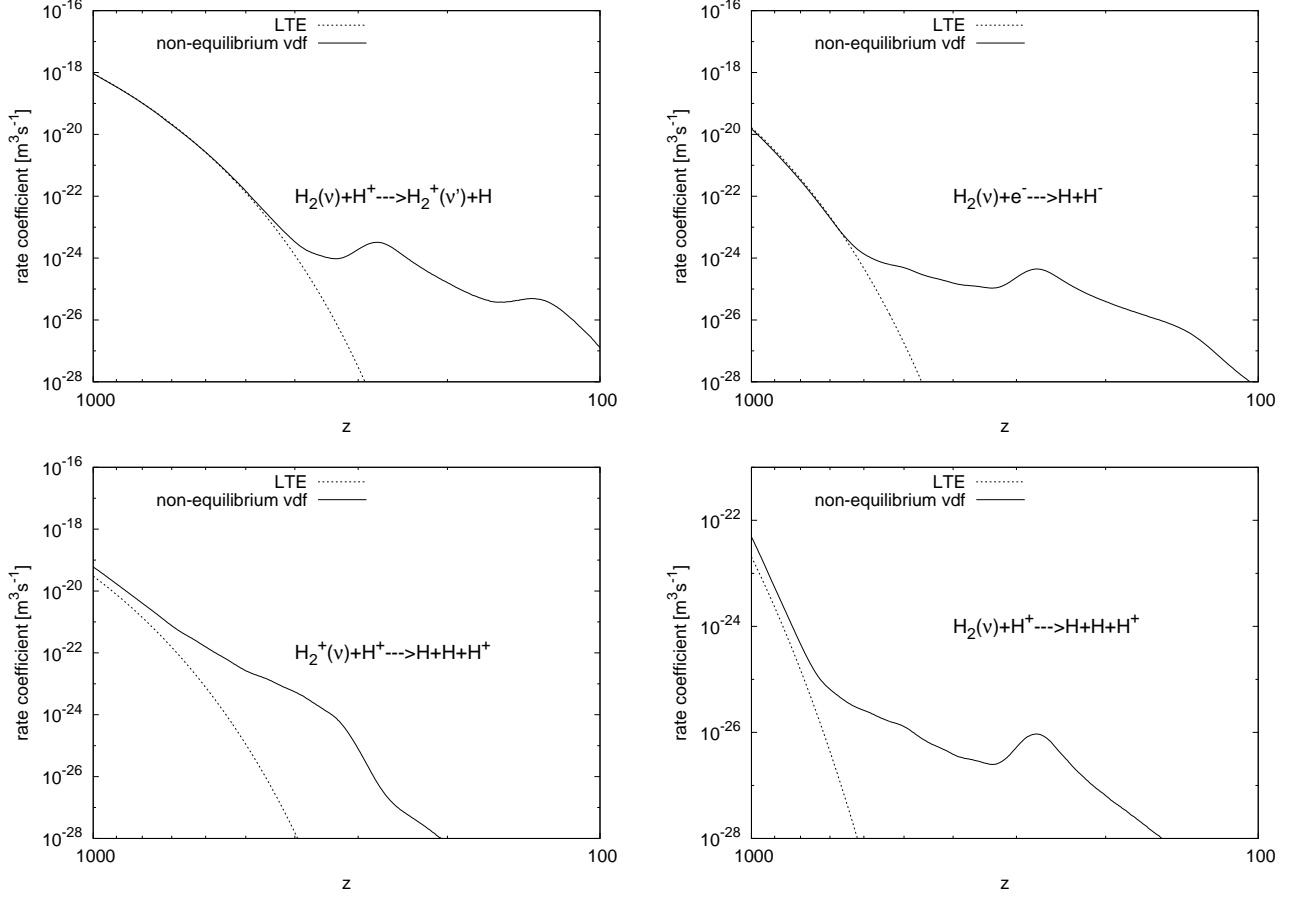
FIG. 5.— Rate coefficients as a function of z: LTE approximation (*dashed line*, fit by Coppola et al. 2011a) and non-equilibrium vibrational distribution function (*solid line*).

5. NON-EQUILIBRIUM REACTION RATES

Using the real non-equilibrium vibrational distributions, vibrationally resolved rate coefficients have been recomputed and compared with the corresponding LTE fits by C11. In Figure 5 the results for the following processes introduced in the model are shown, both for H$_2$ and H$_2^+$: (1) H$_2(v)$/H$^+$ charge transfer (2) H$_2(v)$/e$^-$ dissociative attachment (3) H$_2^+(v)$ dissociation by collisions with H (4) H$_2(v)$ dissociation by collisions with H$^+$. The LTE fit for dissociative attachment of H$_2$ is taken from Capitelli et al. (2007). Strong deviations from the LTE fits can be noted, due to the non-equilibrium pattern, especially at low z, where the hypothesis of Boltzmann distribution of the vibrational level manifold fails. The peak at $z \approx 300$ corresponds to that on H$_2^+$ (and consequently to H$_2$, via the process of charge transfer with H$^+$). It should be noted that, in the case of H$_2$ dissociative attachment, the non-equilibrium calculation follows the trend reported by Capitelli et al. (2007), where a simplified model for the non-equilibrium distribution was assumed.

6. SPECTRAL DISTORTIONS OF THE CBR

The photons created in the H_2 formation process produce a distortion of the black-body spectrum of the cosmic background radiation (CBR). Since the maximum production of H_2 occurs in vibrationally excited states by associative detachment in collisions of H and H^- at redshifts below $z \approx 100$ (see Coppola et al. (2011a)), the emission of rovibrational transitions with wavelength $\lambda \approx 2~\mu m$ is redshifted today at $\lambda \approx 100$–$200~\mu m$, in the Wien part of the CBR. An early estimate of this distortion, based on the rovibrational-resolved associative detachment cross sections computed by Bieniek & Dalgarno (1979), was made by Khersonskii (1982) while Shchekinov & Éntél (1984) developed a model for the molecular hydrogen distortion due to secondary heating processes. We reconsider here the process of vibrational emission of primordial H_2 molecules with our updated chemical network and with a fully kinetic treatment of the level populations of H_2.

For each transition from an upper level v_u to a lower level v_l, with level populations n_u and n_l and degeneracy coefficients g_u and g_l, the relative perturbation in the CBR at the present time is given by

$$\left.\frac{\Delta J_\nu}{J_\nu}\right|_{z=0} = [S(z_{\text{int}}) - 1]\tau(z_{\text{int}}), \qquad (11)$$

where

$$S(z_{\text{int}}) = \left[\frac{g_u n_l(z_{\text{int}})}{g_l n_u(z_{\text{int}})} - 1\right]^{-1} \left\{\exp\left[\frac{h\nu_{ul}}{kT_{\text{r}}(z_{\text{int}})}\right] - 1\right\} \qquad (12)$$

is the source function, and

$$\tau(z_{\text{int}}) = \frac{c^3}{8\pi\nu_{ul}^3} A_{ul} \frac{g_u}{g_l} \left[1 - \frac{g_l n_u(z_{\text{int}})}{g_u n_l(z_{\text{int}})}\right] \frac{n_l(z_{\text{int}})}{H_z(z_{\text{int}})}, \qquad (13)$$

is the redshift-integrated optical depth (see e.g. Appendix A of Bougleux & Galli 1997). In Eqs. (12) and (13), z_{int} is the interaction redshift, at which the observed frequency ν is equal to the redshifted frequency ν_{ul} of the transition, i.e.

$$\nu(1 + z_{\text{int}}) = \nu_{ul}, \qquad (14)$$

A_{ul} are the Einstein coefficients, and H_z is the Hubble function

$$H_z = H_0[\Omega_r(1+z)^4 + \Omega_m(1+z)^3 + \Omega_k(1+z)^2 + \Omega_\Lambda]^{1/2} \qquad (15)$$

(see Coppola et al. (2011a) for a definition of the cosmological constants and their adopted values).

Figure 6 shows the emission produced by H_2 transitions with $\Delta v = 1$, 2, 3 and 4 in the frequency range $\nu = 10$–$1000~cm^{-1}$, corresponding to wavelengths $\lambda = 10~\mu m$–$1~mm$. To avoid confusion, only the first 4 transitions for each Δv are shown (i.e., $v = 1 \to 0$, $2 \to 1$, $3 \to 2$ and $4 \to 3$ for $\Delta v = 1$, etc.). The figure also shows the CBR in the Wien region, and, for comparison, the spectral features produced by the cosmological recombination of H and He (e.g. Chluba & Sunyaev 2007,2008, Chluba, Rubiño-Martín and Sunyaev (2007), Rubiño-Martín, Chluba and Sunyaev (2008)). The latter are mainly formed by redshifted Ly-α and two-photon transitions of H and the corresponding lines from He (Chluba & Sunyaev 2010 have recently produced new results for this last contribution).
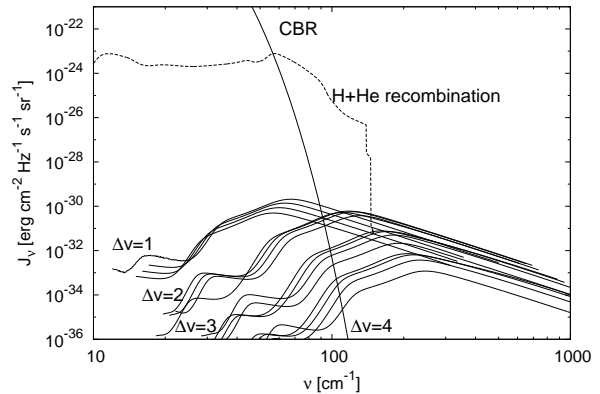

FIG. 6.— CBR spectrum at $z=0$ together with spectral distortions due to H and He recombinations (Chluba, Rubiño-Martín and Sunyaev (2007), Rubiño-Martín, Chluba and Sunyaev (2008)) and to non-equilibrium vibrational molecular transitions for H_2. The contribution of multiquantum transitions up to $\Delta v = 4$ are shown.

The difficulty of detecting spectral distortions in the Wien side of the CBR, in the presence of an infrared background (both Galactic and extragalactic) several orders of magnitude brighter, have been discussed by Wong et al. (2006). While a direct detection appears challenging (see also Schleicher et al. 2008), we stress that an excess of photons over the CBR at wavelengths shorter than the peak could represent a significant contribution to several photodestruction processes, as shown by Switzer & Hirata (2005) for the photoionization of Li and Hirata & Padmanabhan (2006) for the photodetachment of H^-. Another possibility is fluorescence, i.e. the absorption of the short-wavelengths non-thermal photons by atoms or molecules followed by re-emission at longer wavelenghts in the Rayleigh-Jeans region of the CBR, as suggested by Dubrovich & Lipovka (1995). These issues will be addressed elsewhere.

7. CONCLUSIONS

We have considered several vibrational non-equilibrium effects on the chemistry and physics of early Universe. Although our present calculations raise several questions about the very use of the concept of temperature in the early Universe, the most important issue concerning thermal transfer and chemical reactivity has been addressed. Our calculations show that the differences between the excitation, translation and radiation temperatures can affect the heat transfer functions of important species, an effect here demonstrated for H_2. Our results underline the necessity to fully include the consequences of the temperature separations which occur at different epochs in the chemical and physical evolution of the early Universe.

Excitation temperatures appear to be higher than radiation temperature at low z; this "chemical" pre-heating should be considered while modeling the formation of galaxies, together with virialization heating and other physical mechanisms usually suggested (e.g. Mo et al. (2005), Wang & Abel (1996)). We have also assessed the hypothesis of steady-state for the vibrational distribution presenting a reduced kinetic model, and calculated the deviations between vibrational temperatures of ortho- and para- states as a first step towards a full non-equilibrium rotovibrational kinetics. Heat

transfer functions are calculated for both equilibrium and non-equilibrium cases, considering also a novel two-temperatures approach that takes into account the different rates of energy exchange among molecular degrees of freedom. For pure vibrational transitions, the critical density is greater than the baryon density, so that the hypothesis of non-equilibrium is also valid at higher z. Resolving rotations and vibrations gives different results, making the limit for z lower (e.g. for the $(0,2) \rightarrow (0,0)$ transition the critical density is about $\approx 2.7\text{x}10^7$ m^{-3} at $z \approx 500$.)

We have evaluated the effects of vibrational non-equilibrium on reaction rates. A general increase has been pointed out because of the formation of long sovrathermal tail in the vibrational distribution, especially at low z; this evidence should be added to the increase of rate coefficients due to the inclusion of the entire vibrational manifold, that by itself can affect in a deep way the fate of the system modeled (as described by Sethi et al. (2010) for the dissociative attachment process).

We have computed the spectral deviations to the CBR due to the non-equilibrium level populations, considering all the transitions. Although the present Planck experiment and the upcoming James Webb Space Telescope (JWST) are able to detect galaxies at high redshift, a direct observation of this effect is challenging; for this reason, an alternative study of the non-thermal vibrational photons on the photochemical pathways of atomic and molecular kinetic should be undertaken.

REFERENCES

Bieniek, R. J., Dalgarno, A., 1979, ApJ, 228, 635
Bougleux, E. & Galli, D., 1997, MNRAS, 288, 638
Capitelli, M., Coppola, C. M., Diomede, P., Longo, S., 2007, A&A, 470, 811
Chluba, J., Sunyaev, R.A., 2007, A&A, 475, 1, 109
Chluba, J., Sunyaev, R.A., 2008, A&A, 480, 3, 1629
Chluba, J., Sunyaev, R.A., 2010, MNRAS, 402, 2, 1221
Chluba, J., Rubiño-Martín, J. A., Sunyaev, R. A., 2007, MNRAS, 374, 4, 1310
Čížek, M., Horáček, J., Domcke, W., 1998, J. Phys. B: Atom., Molec. & Opt. Phys., 31, 2571
Coppola, C. M., Longo, S., Capitelli, M., Palla, F., Galli, D., 2011, ApJS, 193, 7 (C11)
Coppola, C. M., Lodi, L., Tennyson, J., 2011, MNRAS, 2011, 415, 487
Dubrovich, V. K., Lipovka, A. A., 1995, A&A, 296, 301
Esposito, F., Gorse, C., Capitelli, M., 1999, Chem. Phys. Lett., 303, 636
Esposito, F., Capitelli, M., 2001, Atomic and Plasma-Material Interaction Data for Fusion, 9, 65
Flower D. R., Pineau des Forêts G., 2001, MNRAS, 323, 672
Galli D., Palla F., 1998, A&A, 335, 403 (GP98)
Hirata, C. M., Padmanabhan, N., 2006, MNRAS, 372, 1175
Khersonskii, V. K., Ap&SS, 1982, 88, 21
Kreckel, H., Bruhns, H., Čížek, M., Glover, S. C. O., Miller, K. A., Urbain, X., Savin, D. W., 2010, Sci. 329, 69
Le Bourlot J., Pineau des Forêts G., Flower D. R, MNRAS, 1999, 305, 4, 802
Lepp, S., Shull, J. M., ApJ, 1984, 1, 280, 465
Mo, H. J., Yang, X., C. Van Den Bosch, F., Katz, N., 2005, MNRAS, 363, 4, 1155
Palla, F., Salpeter, E. E., Stahler, S. W., ApJ, 1, 271, 632
Puy D., Alecian G., Le Bourlot J., Léorat J., Pineau des Forêts G., 1993, A&A, 267, 337
Puy, D., Signore, M., A&A, 305, 371
Rubiño-Martín, J. A., Chluba, J., Sunyaev, R. A., 2008, A&A, 485, 2, 377
Schleicher, D. R. G., Galli, D., Palla, F., Camenzind, M., Klessen, R. S., Bartelmann, M., Glover, S. C. O., A&A, 490, 2, 2008, 521
Sethi, S., Haiman, Z., Pandey, K., 2010, ApJ, 721, 615
Shchekinov, Y. A., Éntél, M. B., 1984, Sov. Astron., 28, 3, 270
Switzer, E. R., Hirata, C. M., 2005, Phys. Rev. D, 72, 083002
Wang, P., Abel, T., 2008, ApJ, 672, 752
Wolniewicz, L., Simbotin, I., Dalgarno, A., 1998, ApJS, 115, 293
Wong, W. Y., Seager, S., Scott, D., 2006, MNRAS, 367, 1666